ZC3H4 Regulates Infiltrating Monocytes, Attenuating Pulmonary Fibrosis through IL-10

Yaping Liu
Southeast University
Xinxin Zhang
Southeast University
Jing Wang
Southeast University
Fuhuang Yang
Southeast University
Jie Huang
Southeast University
Mengling Chen
Southeast University
Sha Wang
Southeast University
Wei Zhang
Southeast University
Caolong Li
China Pharmaceutical University
Jie Chao (chaojie@seu.edu.cn)
Southeast University https://orcid.org/0000-0002-7800-3557

Research Article

Keywords: monocytes, ZC3H4, silicosis, autophagy, IL-10

Posted Date: January 19th, 2022

DOI: https://doi.org/10.21203/rs.3.rs-1251889/v1

Abstract

Silicosis is a pulmonary fibrosis-associated disease caused by the inhalation of large amounts of free silicon dioxide (SiO_2) that mainly manifests as early inflammation and late pulmonary fibrosis. As macrophage precursors, monocytes accumulate in the lung during early inflammation, but their role in the development of silicosis is unclear. Single cell sequencing, western blotting, quantitative real-time PCR, ELISA and cell functional experiments were used to explore the specific effects of monocytes on fibroblasts. The CRISPR/Cas9 system was used to specifically knock down ZC3H4 and was combined with pharmacological methods to explore the mechanism by which ZC3H4 affects chemokine and cytokine secretion. The results indicated that 1) SiO_2 induced an infiltrating phenotype in monocytes; 2) infiltrating monocytes inhibited the activation, viability and migration of fibroblasts by regulating IL-10 but not IL-8; and 3) SiO_2 downregulated IL-10 via ZC3H4-induced autophagy. This study revealed that ZC3H4 regulated the secretion function of monocytes, which, in turn, inhibited fibroblast function in early inflammation through autophagy signaling, thereby reducing pulmonary fibrosis. These findings provide a new idea for the clinical treatment of silicosis.

Introduction

Silicosis is a chronic occupational disease caused by long-term inhalation of free silicon dioxide (SiO_2). [1] Silicosis is a potentially fatal, incurable and disabling pulmonary disease that is characterized by silicotic nodule formation and pulmonary interstitial fibrosis.[2] However, as early as 1995, the International Labor Organization (ILO) and World Health Organization (WHO) proposed the "Global Pneumoconiosis International Plan", which aimed to completely eliminate pneumoconiosis by 2030. However, recently, the Lancet suggested that in recent years, the world has failed to prevent and treat pneumoconiosis.[3, 4] Moreover, the incidence and prevalence of silicosis are increasing markedly, and effective therapies are not currently available. Despite a plethora of studies that have investigated the toxicity of crystalline silica over the last several decades, the exact mechanism of silicosis currently remains elusive.

Monocytes are innate immune cells and have functions such as phagocytosis, antigen presentation and inflammation.[5] As macrophage precursor cells, monocytes accumulate in the lungs in the early stage of silicosis, helping to maintain the immune function of macrophages. In humans, monocytes can be divided into three subgroups: the inflammatory type, intermediate type and patrolling type.[6] In inflammatory diseases, patrolling monocytes also induce proinflammatory effects.[7] Bone marrow-derived monocytes accumulate at inflammatory sites along chemokine gradients and exert effects.[8] There have been few studies on the function of monocytes during pulmonary fibrosis, and their functions are still controversial: some scholars believe that the release of TGF-β1 by monocytes inhibits collagen degradation and exacerbates pulmonary fibrosis,[9, 10] and some scholars believe that C-C motif chemokine receptor 2 $(CCR2)^+$ monocytes can inhibit lung fibrosis.[11] These findings strongly suggest that monocytes play a crucial role in silicosis. Our recent studies showed that monocytes, while

mediating an inflammatory response, can also affect the function of fibroblasts. This effect may be a positive way the body responds to early inflammation in silicosis by inhibiting early fibroblast activation to suppress the development of lung fibrosis in the later stage.

At present, the clinical treatment of pulmonary fibrosis is mostly concentrated on macrophages which initiates pulmonary fibrosis via releasing a large number of inflammatory media [12–14] [15], so inhibiting the activation of macrophages can effectively inhibit the development of pulmonary fibrosis. In current study, blocking the conversion of monocytes to macrophages not only inhibits the release of inflammatory factors from macrophages, but also inhibits the release of inflammatory factors from monocytes, indicating early inhibition of inflammatory response is a more effective treatment for pulmonary fibrosis induced by SiO_2. Moreover, we found that ZC3H4 could regulate monocytes by reducing interleukin 10 (IL-10) release to affect fibroblast functions. These findings suggest that monocytes play an important role in the development of silicosis and that ZC3H4 can affect monocytes.

Results

Silica promotes an infiltrating phenotype in monocytes

First, we used single-cell sequencing (sc-Seq) technology to examine whole lungs of mice in the 7-d saline group, 7-d SiO_2 model group, 56-d saline group and 56-d SiO_2 model group by digestion analysis, and all the cell classifications in the mouse lung were obtained (Figure 1A) by R language analysis. Many researchers established pulmonary fibrosis model in mice by endotracheal infusion of silica to further explore the mechanism [16, 17]. The dosage of silica was 5 mg each animal for *in vivo* experiments which was based upon previous studies and simulated acute high-dose exposure in an occupational environment.[18] The number of monocytes in the 7-d SiO_2 model group was not significantly different from the number of monocytes in the 7-d saline group, while the number of macrophages in the 7-d SiO_2 model group was elevated. The number of monocytes in the 56-d SiO_2 model group was significantly lower than that in the 56-d saline group, while the number of macrophages was elevated in the 56-d SiO_2 model group (Figure 1B and C). After pseudochronological analysis, the increased macrophages were shown to be transdifferentiated from monocytes (Figure 1D). Many studies have shown that alveolar macrophages play an important role in the process of fibroblast activation and the development of silicosis.[19, 20] As macrophage precursor cells, monocytes are recruited in large numbers during silicosis, but their effects are still unclear. To determine whether SiO_2 affects the monocyte phenotype, the THP-1 cell line was exposed to SiO_2 (100 μg/ml), and phenotypic changes were assessed. Interestingly, the immunoblotting results (Figure 1E and F) showed that SiO_2 upregulated CCR2 but not integrin subunit alpha X (ITGAX, CD11C, Figure 1E and G) or adhesion G protein-coupled receptor E1 (ADGRE1, F4/80, Figure 1E), suggesting that the infiltrating monocyte phenotype increased. This finding was further confirmed by immunostaining analysis of CCR2 in THP-1 cells (Figure 1H) compared to that in the control groups, indicating that transdifferentiation from monocytes to macrophages was blocked, which was

contrary to the sc-Seq results. Therefore, it is worth exploring the role of infiltrating monocytes in the process of fibrosis.

Monocytes play a negative role in fibroblast activation, migration and viability after silica treatment

Lung fibroblasts, which are the direct effector cells of pulmonary fibrosis, gradually transform into myofibroblasts during the progression of silicosis.[21] To determine whether infiltrating monocytes affect fibroblast activation, we treated the HPF-a cell line with conditioned medium monocytes treated with SiO_2 (CM) or PBS (Con). The immunoblotting results demonstrated that compared to Con, CM inhibited the expression of the fibroblast activation marker proteins COL1A1 and ACTA2 (Figure 2A-C). To determine whether infiltrating monocytes affect fibroblast viability, HPF-a cells were cultured in CM or Con. As the gel contraction assay results indicated, the CM groups exhibited less cell viability than the Con group (Figure 2D and E). Moreover, the CCK-8 assay results showed that CM inhibited fibroblast viability compared with that in the control group (Figure 2F), which confirms the gel contraction assay results. Considerable evidence has suggested that pulmonary fibroblast migration is one main cause of pulmonary fibrosis. We examined whether infiltrating monocytes affected fibroblast migration. The results of the scratch assay (Figure 2G and H) show that SiO_2 promoted the migration of HPF-a cells. Taken together, these results suggested that monocyte exposure to SiO_2 exerted a protective effect against fibrosis.

Increased IL-8 expression is not a key factor that affects fibroblast activation, viability or migration

To further investigate which cytokines influence the functions of fibroblasts, we examined several factors. First, we measured the classic cytokine TGF-β1[22, 23] and found that the mRNA level was not changed after SiO_2 stimulation (Figure 3A). Then, we measured 12 inflammation-related cytokines by ELISA and found that IL-8 expression showed an increasing trend (Figure 3B). To confirm whether IL-8 was increased by SiO_2, we measured its mRNA and protein expression. The results showed that IL-8 mRNA expression (Figure 3C) and IL-8 protein levels increased (Figure 3D) in the THP-1 cell line after SiO_2 stimulation. To identify whether IL-8 was the main factor in CM that affected fibroblasts, we added IL-8 to normal medium. Interestingly, both ACTA2 and COL1A1 were significantly increased after IL-8 treatment (Figure 3E-G). In addition, IL-8 also promoted fibroblast viability (Figure S1). The 2D scratch assay was used to evaluate migration, and IL-8 promoted cell migration, as expected (Figure 3H and I).

Decreased IL-10 release is a key factor that affects fibroblast activation, viability and migration

After examining the effect of IL-8, we found that it was inconsistent with the effect of CM; thus, we reviewed the previous data and shifted our focus to the decreased fibrogenic factor IL-10[20, 24, 25]

(Figure 3B). We analyzed the differentially expressed genes in monocyte populations by single-cell sequencing and found that the expression of IL-10 receptors was decreased in the model group (Figure 4A). To confirm that the change in IL-10 was induced by SiO_2, we measured IL-10 protein levels and found a time-dependent decrease in response to SiO_2 stimulation (Figure 4B). To further determine the role of IL-10, we added IL-10 to CM. As expected, the fibroblast activation marker proteins ACTA2 and COL1A1 were both restored after the addition of IL-10 to CM (Figure 4C-E). In addition, IL-10 promoted the migration of HPF-a cells compared to those treated with CM (Figure 4F and G). In addition, the CCK-8 assay (Figure 4H) and gel contraction assay (Figure 4I and J) results indicated that IL-10 could abrogate the negative effects of CM on HPF-a cell viability.

Autophagy is involved in the silica-induced reduction in IL-10 release by monocytes

Based on these results, we showed that the cytokine that affected fibroblast function was IL-10, but how silica regulated the release of IL-10 by THP-1 cells was unclear. To determine what affected the expression of IL-10, we first measured the mRNA level of IL-10. Unexpectedly, the results demonstrated that IL-10 mRNA levels did not show significant changes (Figure 5A). Based on a literature review, we initially thought that there might be a posttranslational modification that regulates IL-10 expression. First, we were concerned that endoplasmic reticulum (ER) stress could control the release of cytokines to a certain extent.[26, 27] To verify our hypothesis, we used Western blotting to analyze ER stress markers, but there was no significant difference in the expression of the marker proteins HSPA5 and DDIT3 (Figure S2A-C). Then, we moved to the autophagy pathway, which is highly associated with cytokine release.[28, 29] We obtained a string map (Figure 5B) and bubble map (Figure 5C) through biological information technology and found that IL-10 played an important role in autophagy signaling pathways. To explore whether autophagy regulated the expression of IL-10, we first measured the expression of autophagy markers. The immunoblotting results showed upregulation of the markers MAP1LC3B, BECN1 and ATG5 (Figure 5D and E). Furthermore, after using the autophagy inhibitor 3-MA to block autophagy, the SiO_2-induced decrease in IL-10 release was significantly inhibited, and the IL-10 protein level was restored (Figure 5F). Moreover, after using the autophagy agonist rapamycin, IL-10 showed a further decline in the SiO_2 treatment group (Figure 5G). Notably, the level of IL-10 decreased in the PBS group after drug administration, which may be due to the nonspecific effect of the drug on cell viability (Figure S3A and B).

ZC3H4 regulates the silica-induced release of IL-10 by monocytes

Previous studies in our laboratory have shown that the zinc finger proteins MCPIP1 (ZC3H12A) and ZC3H4 play important roles in the process of fibrosis caused by the inflammatory response in macrophages.[20, 30] Whether the zinc finger protein ZC3H4 is involved in the effect of monocytes on fibrosis is unclear. To identify whether ZC3H4 is involved in monocytes, we first measured ZC3H4 protein

levels. The immunoblotting results showed that ZC3H4 was significantly increased after SiO_2 treatment (Figure 6A and B). Immunostaining also confirmed this effect (Figure 6C). CRISPR/Cas9 technology (Figure 6D and E) was used to knock down the ZC3H4 protein (NIC). Moreover, ZC3H4-NIC upregulated the IL-10 expression level to that of the control group in the presence of SiO_2 (Figure 6F).

ZC3H4 regulates IL-10 release through autophagic processes

Based on these findings, the results showed that ZC3H4 and autophagy could both regulate the expression of IL-10. According to the literature, there are associations between various zinc finger proteins and autophagy. To verify the relationship between ZC3H4 and autophagy, we knocked down ZC3H4 and observed changes in autophagy marker proteins. The results suggested that the autophagy-related proteins MAP1LC3B, BECN1, and ATG5 were all decreased in the SiO_2 group (Figure 7A-C). To further validate this result, THP-1 cells were transduced with dual fluorescent mRFP-GFP-MAP1LC3 adenovirus to detect autophagy by monitoring autophagosome formation in real time with fluorescence microscopy. mRFP was used to label and track LC3, whereas GFP fluorescence is sensitive to acidic conditions; thus, GFP fluorescence will be quenched when a lysosome and an autophagosome form an autolysosome. SiO_2 significantly induced autophagic flux, and this effect of SiO_2 was attenuated by knocking down ZC3H4 (Figure 7D and F). Moreover, after knocking down ZC3H4, rapamycin reduced the expression of IL-10 under SiO_2 stimulation compared to the effect of no rapamycin.

Discussion

Alveolar macrophages are a particular group of macrophages within lung tissue that respond to particles that are inhaled through the pulmonary bronchial airway via intricate interactions with other cells, such as fibroblasts and epithelial cells.[31] These macrophages function as effector cells by secreting and releasing factors that attract and regulate other cells, resulting in continuous increases in mesenchymal components.[32] Many efforts have been made to prevent fibrosis in the context of silicosis. However, no effective therapies or drugs are currently available to prevent or minimize the progression of SiO_2-induced inflammation.

As macrophage precursor cells, monocytes are innate immune cells that have functions such as phagocytosis, antigen presentation and inflammation.[5] Bone marrow-derived monocytes accumulate in the inflammatory site along chemokine gradients, thereby promoting inflammation. The cell group classifications obtained by single-cell sequencing showed that monocytes differentiated into macrophages through processes that were affected by silicone. However, when we stimulated monocytes directly with SiO_2, monocytes were converted to the $CCR2^+$ inflammatory phenotype and did not differentiate into macrophages. This result led us focus to on $CCR2^+$ monocytes. Blocking of transformation from monocytes to macrophages reduces the secretion of inflammatory factors, inhibits the activation of fibroblasts, and plays a protective role. To date, extensive evidence indicates that $CCR2^+$

cells can promote fibrosis in the lungs. One study suggested that $CCR2^+$ monocytic myeloid-derived suppressor cells (M-MDSCs) inhibited collagen degradation and promoted lung fibrosis by producing TGF-β1.[10] However, our results indicated that infiltrating monocytes inhibited fibroblast activation, viability and migration. Notably, many studies have suggested that macrophages are the main effector cells that cause pulmonary fibrosis, and blocking or reducing macrophages could attenuate pulmonary fibrosis.[33–36] Based on previous studies and experimental results, we hypothesized that regulating monocyte differentiation may be an effective strategy for inhibiting inflammation and fibrosis. Interfering with monocyte differentiation could, on the one hand, suppress the inflammatory cascade; on the other hand, undifferentiated monocytes could directly play a beneficial role by inhibiting inflammation and fibrosis. If the above hypotheses are confirmed, they will provide new ideas for the treatment of silicosis.

IL-10 is widely expressed in a variety of immune cells and is known as an anti-inflammatory cytokine that can inhibit the expression of a variety of inflammatory factors.[37–39] However, studies have suggested that the long-term release of large amounts of IL-10 exacerbates the progression of silicosis.[24, 25, 40] In our study, we found that the release of IL-10 by infiltrating monocytes was decreased, which partly restrained fibroblast functions. Accordingly, inhibiting fibroblast activation in the early inflammation stage may result in weakening lung fibrosis in later stages.

Autophagy, which is an evolutionarily conserved and catabolically driven cytoprotective process, is associated with many physiological processes, including immune cell responses to endogenous and exogenous pathogenic stimuli.[41–44] Our recent study suggested that autophagy plays a major role in determining cellular fate in silicosis.[20, 21] Furthermore, autophagy can regulate the release of various cytokines, including IL-1α, IL-1β, and IL-18.[29, 45, 46] In our study, we found that autophagy could affect the expression of IL-10 via ZC3H4, which is a new type of zinc finger protein whose structure is unclear. In previous studies, ZC3H4 promoted macrophage activation and therefore affected downstream fibroblasts,[30] and ZC3H4 was also involved in epithelial-mesenchymal transition (EMT).[47] In this study, we found that ZC3H4 could regulate the autophagy pathway to inhibit IL-10 release in monocytes, indicating the complicated and key role of ZC3H4 in pulmonary fibrosis.

In summary, our study revealed that infiltrating monocytes could inhibit fibroblast activation, viability and migration and then inhibit lung fibrosis, suggesting early inhibition of inflammatory response is a more effective treatment for silicosis. Additionally, ZC3H4 is a crucial protein associated with silicosis that can regulate IL-10 release by controlling autophagy in monocytes. Consequently, the regulation of monocyte differentiation might be a potential therapeutic strategy for inhibiting inflammation and fibrosis and would bring new opportunities for the treatment of silicosis (Figure 8).

Materials And Methods

Reagents

SiO_2, which has a diameter of approximately 2-5 μm, was purchased from Sigma (S5631). The silica was sterilized overnight (200°C for 16 h)[48] and then dissolved in sterile normal saline (NS) at a concentration of 5 mg/ml. The dose of SiO_2 used *in vivo* and *in vitro* was based on previous studies.[30] Antibodies against α-SMA (14395-1-AP, rabbit), CCR2 (16153-1-AP, rabbit), BECN (11306-1-AP, rabbit), ATG5 (60061-1-Ig, mouse) and LC3 (14600-1-AP, rabbit) were obtained from ProteinTech, Inc. Antibodies against collagen I (BS1530, rabbit) and GAPDH (MB001, mouse) were obtained from BioWorld, Inc.

Animals

C57BL/6 mice (6-8 weeks old) were obtained from Dr. Tao Cheng at Nanjing Medical University Laboratories (Nanjing, China). All animals were male and housed (4 per cage) in a temperature-controlled room (25°C, 50% relative humidity) with a 12-h light/dark cycle. All animal procedures were performed in strict accordance with ARRIVE guidelines, and animal protocols were approved by the Institutional Animal Care and Use Committee of Southeast University.

Single cell sequencing

1. Sample collection
For the model group, mice with significant lesions on CT were included. Lesions were removed from the lungs of mice representing the NS-7d, SiO_2-7d, NS-56d, and SiO_2-56d groups and were used for single-cell sequencing. Each lung was removed in 2 min and quickly washed in precooled PBS 3 times.

2. Single-Cell RNA Sequencing

2.1 Cell capture and cDNA synthesis

Using a single-cell ‘5’ Library and Gel Bead Kit (10x Genomics, 1000169) and Chromium Single-Cell G Chip Kit (10x Genomics, 1000120), the cell suspension (300-600 living cells per microliter determined by Countstar) was loaded onto a Chromium single-cell controller (10x Genomics) to generate single-cell gel beads in the emulsion according to the manufacturer’s protocol. In short, single cells were suspended in PBS containing 0.04% BSA. Approximately 20,000 cells were added to each channel, and the target cell recovered was estimated to be approximately 10,000 cells. Captured cells were lysed, and the released RNA was barcoded through reverse transcription in individual GEMs. Reverse transcription was performed on a S1000TM Touch Thermal Cycler (Bio Rad) at 53°C for 45 min, followed by 85°C for 5 min, and hold at 4°C. cDNA was generated and then amplified, and quality was assessed using an Agilent 4200 (performed by CapitalBio Technology, Beijing).

2.2 Single cell RNA-Seq library preparation

According to the manufacturer’s instructions, single-cell RNA-seq libraries were constructed using the Single Cell 5’ Library and Gel Bead Kit, Single Cell V(D)J Enrichment Kit, Human T Cell (1000005) and Single Cell V(D)J Enrichment Kit. The libraries were finally sequenced using an Illumina NovaSeq6000

sequencer with a sequencing depth of at least 100,000 reads per cell with a paired-end 150 bp (PE150) reading strategy (performed by CapitalBio Technology, Beijing).

3. Data preprocessing

3.1 Cell Ranger pipeline

Cell Ranger software (v.4.0.0) was obtained from the 10x Genomics website https://support.10xgenomics.com/single-cell-gene-expression/software/downloads/latest. Pipeline coupled with mouse reference version mm10. Alignment, filtering, barcode counting, and UMI counting were performed with the Cell Ranger count module to generate a feature-barcode matrix and determine clusters. Dimensionality reduction was performed using PCA, and the first ten principal components were used to generate clusters by the K-means algorithm and graph-based algorithm.

3.2 DEGs identification and Enrichment Analysis

Differentially expressed genes were analyzed using sc-Seq with negative binomial models to estimate the false discovery rate (FDR). For each cluster, genes with adjusted $\log_2$-fold change >3 and $P < 0.001$ were considered significantly upregulated. GO enrichment and KEGG enrichment of cluster markers were performed using the R package clusterProfiler, using the top significantly upregulated genes of each cluster. The results were visualized using R package.

3.3 Cell Type Annotation

Cell type was annotated by Cell Marker.

Isolation of mouse primary monocytes

Cells were collected from mouse bone marrow, treated with ACK lysis buffer, and routinely maintained in RPMI (10% FBS, 1% penicillin/streptomycin) at 37°C with 5% CO_2. The suspension cells were transferred into new medium for one day as the experiment required.

Cell culture

The THP-1 cell line was purchased from ATCC®, routinely maintained in RPMI (10% FBS, 1% penicillin/streptomycin) and incubated at 37°C and 5% CO_2. HPF-a cells were purchased from ATCC®, routinely maintained in DMEM (10% FBS, 1% penicillin/streptomycin) and incubated at 37°C and 5% CO_2.

Western blot analysis

Cells were collected in polyethylene tubes and briefly washed with ice-cold phosphate-buffered saline (PBS) twice before being lysed. The protein concentrations of the lysates were measured with a bicinchoninic acid (BCA) kit (Beyotime, China), and 30 μg of total protein was resolved via SDS-PAGE. Then, the proteins were transferred onto a polyvinylidene difluoride (PVDF) membrane. The membrane was blocked with 5% nonfat dry milk in Tris-buffered saline with Tween-20 (TBST) for 1 h and then

incubated overnight (16 h) with primary antibodies against Col1A1, α-SMA, CHOP, BIP, BECN, ATG5 and LC3B (1:1000). After being washed with TBST, the membrane was incubated for 1 h with secondary antibodies conjugated to horseradish peroxidase. Protein bands were visualized using a chemiluminescence detection system. All Western blots are representative of three or more independent experiments. The protein bands were quantified using ImageJ 1.52v software.

Cell viability assay

Cell viability was measured using CCK-8 assays. Briefly, the cells were seeded in 96-well plates at a density of 1×10^5 cells/well (for THP-1 cells) or 5×10^4 cells/well (for HPF-a cells). The cells were treated with conditioned media for 24 h (for HPF-a cells) or with 3-MA or rapamycin for 24 h (for THP-1 cells). The cells were then exposed to CCK-8 solution (10 μL), and the plates were incubated for an additional 30 min to 4 h. The absorption values were measured at 450 nm.

Immunocytochemistry

Cells were fixed with 4% paraformaldehyde in PBS on ice for 2 h. The fixed samples were permeabilized for 30 min at room temperature (RT) in PBS containing 0.3% Triton X-100 (PBST) and then blocked with 10% normal goat serum (NGS; Life Technologies) in PBST at RT for 2 h. The blocked samples were incubated for 4 h on ice with primary antibodies diluted in PBST plus 10% NGS. The samples were then washed three times with PBS and incubated with donkey anti-rabbit (conjugated to Alexa Fluor® 488) and donkey anti-mouse (conjugated to Alexa Fluor® 576) secondary antibodies for 2 h at RT. After being washed three times in PBS, the samples were mounted with Prolong® Gold antifade reagent containing DAPI, and the slides were examined using a fluorescence microscope.

Detection of autophagic flux

THP-1 cells were seeded in 6-well plates and transfected with mRFP-green fluorescent protein (GFP)-LC3 adenoviral vectors according to the manufacturer's instructions (HanbioInc, Shanghai, CN, USA). Successfully transfected cells expressed LC3 protein tagged with RFP and GFP. GFP is acid-sensitive, and the green fluorescence is quenched in the acidic environment of a lysosome. However, in contrast, RFP is relatively stable within lysosomes. Therefore, the numbers of GFP and RFP puncta were examined and quantified by confocal microscopy. The red and yellow (i.e., a combination of red and green) spots indicate autophagosomes and autolysosomes, respectively.[49]

Scratch assay

HPF-a cells were treated with conditioned media, IL-8 or IL-10 for 48 h in 24-well plates. To assess fibroblast motility, a scratch assay was performed as previously described.[50]

Real-time PCR

Total RNA was isolated from cells and subjected to reverse transcription using a Prime Script RT master mix kit (TaKaRa, RR036). Real-time PCR was performed by a StepOne^{TM} Real-Time PCR System (Life Technologies, 4376357, Singapore) using primers for human IL-10 (forward primer: 5'-

GTGATGCCCCAAGCTGAGA-3’; reverse primer: 5’-CACGGCCTTGCTCTTGTTT -3’) and human IL-8 (forward primer: 5’-CTGATTTCTGCAGCTCTGTG-3’; reverse primer: 5’-GGGTGGAAAGGTTTGGAGTATG-3’).

ELISA

Twelve inflammatory cytokines were analyzed by Human Inflammatory Cytokines Multi-Analyte ELISArray™ Kits (QIAGEN, MEH-004A). Human IL-10 and human IL-8 ELISA kits were purchased from JinYiBai® (Nanjing, China). All cytokines were measured according to the manufacturer’s protocol.

Statistical analysis

The data were analyzed using GraphPad Prism 5.0 (GraphPad Software, Inc.). Unpaired numerical data were analyzed by unpaired Student’s t-tests (2 groups) or ANOVA (2 groups). The level of significance was set at 0.05; values of $P<0.05$ indicated statistical significance.

Declarations

Acknowledgments

This study was completed with the support of the Medical School of Southeast University.

Funding

National Natural Science Foundation of China 81972987 and 81773796.

National Key R&D Program of China 2017YFA0104303.

Postgraduate Research and Practice Innovation Program of Jiangsu Province.

Author contributions

L.Y., Z.X., W.J, and Y.F. performed the experimental work, interpreted the data, prepared the figures and wrote the manuscript. H.J., C.M. and S.W performed the experiments and interpreted the data. L.C. and Z.W. designed and performed the experiments and interpreted the data. J.C. provided the funding and laboratory space and designed and monitored all the experiments. All the authors carefully read, discussed and approved the final manuscript.

Declaration of interests

The authors have no conflicts of interest to declare.

References

1. Lee S, Hayashi H, Mastuzaki H, Kumagai-Takei N, Otsuki T. Silicosis and autoimmunity. Current opinion in allergy and clinical immunology. 2017;17(2):78–84. doi: 10.1097/ACI.0000000000000350.

2. Fernandez Alvarez R, Martinez Gonzalez C, Quero Martinez A, Blanco Perez JJ, Carazo Fernandez L, Prieto Fernandez A. Guidelines for the diagnosis and monitoring of silicosis. Archivos de bronconeumologia. 2015;51(2):86–93. doi: 10.1016/j.arbres.2014.07.010.

3. The Lancet Respiratory Medicine. The world is failing on silicosis. Lancet Respir Med. 2019;7(4):283. doi: 10.1016/s2213-2600(19)30078-5.

4. Kirby T. Australia reports on audit of silicosis for stonecutters. Lancet. 2019;393(10174):861.

5. Florentin J, Coppin E, Vasamsetti SB, Zhao J, Tai YY, Tang Y, et al. Inflammatory macrophage expansion in pulmonary hypertension depends upon mobilization of blood-borne monocytes. J Immunol. 2018;200(10):3612–25. doi: 10.4049/jimmunol.1701287.

6. Jacquelin S, Licata F, Dorgham K, Hermand P, Poupel L, Guyon E, et al. CX3CR1 reduces Ly6Chigh-monocyte motility within and release from the bone marrow after chemotherapy in mice. Blood. 2013;122(5):674–83. doi: 10.1182/blood-2013-01-480749.

7. Mukherjee R, Kanti Barman P, Kumar Thatoi P, Tripathy R, Kumar Das B, Ravindran B. Non-classical monocytes display inflammatory features: validation in sepsis and systemic lupus erythematous. Sci Rep. 2015;5:13886. doi: 10.1038/srep13886.

8. Serbina NV, Pamer EG. Monocyte emigration from bone marrow during bacterial infection requires signals mediated by chemokine receptor CCR2. Nat Immunol. 2006;7(3):311–7.

9. Groves AM, Johnston CJ, Williams JP, Finkelstein JN. Role of infiltrating monocytes in the development of radiation-induced pulmonary fibrosis. Radiation research. 2018;189(3):300–11. doi: 10.1667/RR14874.1.

10. Lebrun A, Lo Re S, Chantry M, Izquierdo Carerra X, Uwambayinema F, Ricci D, et al. $CCR2^{+}$ monocytic myeloid-derived suppressor cells (M-MDSCs) inhibit collagen degradation and promote lung fibrosis by producing transforming growth factor-beta1. The Journal of pathology. 2017;243(3):320–30. doi: 10.1002/path.4956.

11. Gurczynski SJ, Procario MC, O'Dwyer DN, Wilke CA, Moore BB. Loss of CCR2 signaling alters leukocyte recruitment and exacerbates gamma-herpesvirus-induced pneumonitis and fibrosis following bone marrow transplantation. American journal of physiology Lung cellular and molecular physiology. 2016;311(3):L611–L27. doi: 10.1152/ajplung.00193.2016.

12. Huang J, Maier C, Zhang Y, Soare A, Dees C, Beyer C, et al. Nintedanib inhibits macrophage activation and ameliorates vascular and fibrotic manifestations in the Fra2 mouse model of systemic sclerosis. Ann Rheum Dis. 2017;76(11):1941-8. doi: 10.1136/annrheumdis-2016-210823.

13. Li Y, Bao J, Bian Y, Erben U, Wang P, Song K, et al. S100A4(+) Macrophages Are Necessary for Pulmonary Fibrosis by Activating Lung Fibroblasts. Front Immunol. 2018;9:1776. doi: 10.3389/fimmu.2018.01776.

14. Meziani L, Mondini M, Petit B, Boissonnas A, Thomas de Montpreville V, Mercier O, et al. CSF1R inhibition prevents radiation pulmonary fibrosis by depletion of interstitial macrophages. Eur Respir J. 2018;51(3). doi: 10.1183/13993003.02120-2017.

15. Wang X, Zhang Y, Zhang W, Liu H, Zhou Z, Dai X, et al. MCPIP1 Regulates Alveolar Macrophage Apoptosis and Pulmonary Fibroblast Activation After in vitro Exposure to Silica. Toxicol Sci. 2016;151(1):126-38. doi: 10.1093/toxsci/kfw029.

16. Huang J, Huang J, Ning X, Luo W, Chen M, Wang Z, et al. CT/NIRF dual-modal imaging tracking and therapeutic efficacy of transplanted mesenchymal stem cells labeled with Au nanoparticles in silica-induced pulmonary fibrosis. J Mater Chem B. 2020;8(8):1713-27. doi: 10.1039/c9tb02652e.

17. Lopes-Pacheco M, Ventura TG, de Oliveira HD, Moncao-Ribeiro LC, Gutfilen B, de Souza SA, et al. Infusion of bone marrow mononuclear cells reduces lung fibrosis but not inflammation in the late stages of murine silicosis. PLoS One. 2014;9(10):e109982. doi: 10.1371/journal.pone.0109982.

18. Bandeira E, Oliveira H, Silva JD, Menna-Barreto RFS, Takyia CM, Suk JS, et al. Therapeutic effects of adipose-tissue-derived mesenchymal stromal cells and their extracellular vesicles in experimental silicosis. Respir Res. 2018;19(1):104. doi: 10.1186/s12931-018-0802-3.

19. Liu H, Zhang H, Forman HJ. Silica induces macrophage cytokines through phosphatidylcholine-specific phospholipase C with hydrogen peroxide. American journal of respiratory cell and molecular biology. 2007;36(5):594–9. doi: 10.1165/rcmb.2006-0297OC.

20. Liu F, Dai W, Li C, Lu X, Chen Y, Weng D, et al. Role of IL-10-producing regulatory B cells in modulating T-helper cell immune responses during silica-induced lung inflammation and fibrosis. Sci Rep. 2016;6(1):1–12.

21. Chu H, Wang W, Luo W, Zhang W, Cheng Y, Huang J, et al. CircHECTD1 mediates pulmonary fibroblast activation HECTD1. Ther Adv Chronic Dis. 2019;10:2040622319891558. doi: 10.1177/2040622319891558.

22. Li N, Feng F, Wu K, Zhang H, Zhang W, Wang W. Inhibitory effects of astragaloside IV on silica-induced pulmonary fibrosis via inactivating TGF-β1/Smad3 signaling. Biomed Pharmacother. 2019;119:109387. doi: 10.1016/j.biopha.2019.109387.

23. Song ZS, Shao H, Chen YQ, Zhang R. Expression and significance of NLRP3/IL-1β/TGF-β(1) signal axis in rat model of silicosis pulmonary fibrosis. Zhonghua Lao Dong Wei Sheng Zhi Ye Bing Za Zhi. 2018;36(11):819–23. doi: 10.3760/cma.j.issn.1001-9391.2018.11.005.

24. Barbarin V, Arras M, Misson P, Delos M, McGarry B, Phan SH, et al. Characterization of the effect of interleukin-10 on silica-induced lung fibrosis in mice. American journal of respiratory cell and molecular biology. 2004;31(1):78–85.

25. Barbarin V, Xing Z, Delos M, Lison D, Huaux F. Pulmonary overexpression of IL-10 augments lung fibrosis and Th2 responses induced by silica particles. American journal of physiology Lung cellular and molecular physiology. 2005;288(5):L841–L8.

26. Roberson EC, Tully JE, Guala AS, Reiss JN, Godburn KE, Pociask DA, et al. Influenza induces endoplasmic reticulum stress, caspase-12-dependent apoptosis, and c-Jun N-terminal kinase-mediated transforming growth factor-β release in lung epithelial cells. American journal of respiratory cell and molecular biology. 2012;46(5):573–81. doi: 10.1165/rcmb.2010-0460OC.

27. Cheng L, Zhao H, Zhang W, Liu B, Liu Y, Guo Y, et al. Overexpression of conserved dopamine neurotrophic factor (CDNF) in astrocytes alleviates endoplasmic reticulum stress-induced cell damage and inflammatory cytokine secretion. Biochem Biophys Res Commun. 2013;435(1):34–9. doi: 10.1016/j.bbrc.2013.04.029.

28. Bursch W, Karwan A, Mayer M, Dornetshuber J, Fröhwein U, Schulte-Hermann R, et al. Cell death and autophagy: cytokines, drugs, and nutritional factors. Toxicology. 2008;254(3):147–57.

29. Harris J. Autophagy and cytokines. Cytokine. 2011;56(2):140–4.

30. Yang X, Wang J, Zhou Z, Jiang R, Huang J, Chen L, et al. Silica-induced initiation of circular ZC3H4 RNA/ZC3H4 pathway promotes the pulmonary macrophage activation. FASEB J. 2018;32(6):3264–77.

31. Mir SUR, Jin L, Craven RJ. Neutrophil gelatinase-associated lipocalin (NGAL) expression is dependent on the tumor-associated sigma-2 receptor S2RPgrmc1. J Biol Chem. 2012;287(18):14494–501. doi: 10.1074/jbc.M111.324921.

32. Hussell T, Bell TJ. Alveolar macrophages: plasticity in a tissue-specific context. Nat Rev Immunol. 2014;14(2):81–93. doi: 10.1038/nri3600.

33. Joshi N, Watanabe S, Verma R, Jablonski RP, Chen CI, Cheresh P, et al. A spatially restricted fibrotic niche in pulmonary fibrosis is sustained by M-CSF/M-CSFR signalling in monocyte-derived alveolar macrophages. Eur Respir J. 2020;55(1):1900646. doi: 10.1183/13993003.00646-2019.

34. Cui H, Jiang D, Banerjee S, Xie N, Kulkarni T, Liu RM, et al. Monocyte-derived alveolar macrophage apolipoprotein E participates in pulmonary fibrosis resolution. JCI Insight. 2020;5(5):e134539. doi: 10.1172/jci.insight.134539.

35. Shichino S, Abe J, Ueha S, Otsuji M, Tsukui T, Kosugi-Kanaya M, et al. Reduced supply of monocyte-derived macrophages leads to a transition from nodular to diffuse lesions and tissue cell activation in

silica-induced pulmonary fibrosis in mice. Am J Pathol. 2015;185(11):2923–38. doi: 10.1016/j.ajpath.2015.07.013.

36. Moore BB, Paine R, Christensen PJ, Moore TA, Sitterding S, Ngan R, et al. Protection from pulmonary fibrosis in the absence of CCR2 signaling. J Immunol. 2001;167(8):4368–77. doi: 10.4049/jimmunol.167.8.4368.

37. Couper KN, Blount DG, Riley EM. IL-10: the master regulator of immunity to infection. J Immunol. 2008;180(9):5771–7.

38. Fiorentino DF, Zlotnik A, Mosmann TR, Howard M, O'garra A. IL-10 inhibits cytokine production by activated macrophages. J Immunol. 1991;147(11):3815–22.

39. De Waal Malefyt R, Abrams J, Bennett B, Figdor CG, De Vries JE. Interleukin 10 (IL-10) inhibits cytokine synthesis by human monocytes: an autoregulatory role of IL-10 produced by monocytes. J Exp Med. 1991;174(5):1209–20.

40. Huaux F, Louahed J, Hudspith B, Meredith C, Delos M, Renauld JC, et al. Role of interleukin-10 in the lung response to silica in mice. American journal of respiratory cell and molecular biology. 1998;18(1):51–9.

41. Qian M, Fang X, Wang X. Autophagy and inflammation. Clin Transl Med. 2017;6(1):24.

42. Rabinowitz JD, White E. Autophagy and metabolism. Science. 2010;330(6009):1344–8.

43. Levine B, Kroemer G. Autophagy in the pathogenesis of disease. Cell. 2008;132(1):27–42.

44. Mizushima N. Autophagy: process and function. Genes Dev. 2007;21(22):2861–73.

45. Ge Y, Huang M, Yao YM. Autophagy and proinflammatory cytokines: interactions and clinical implications. Cytokine & growth factor reviews. 2018;43:38–46. doi: 10.1016/j.cytogfr.2018.07.001.

46. Harris J, Hartman M, Roche C, Zeng SG, O'Shea A, Sharp FA, et al. Autophagy controls IL-1β secretion by targeting pro-IL-1β for degradation. J Biol Chem. 2011;286(11):9587–97.

47. Jiang R, Zhou Z, Liao Y, Yang F, Cheng Y, Huang J, et al. The emerging roles of a novel CCCH-type zinc finger protein, ZC3H4, in silica-induced epithelial to mesenchymal transition. Toxicology letters. 2019;307:26–40. doi: 10.1016/j.toxlet.2019.02.014.

48. Zhou Z, Jiang R, Yang X, Guo H, Fang S, Zhang Y, et al. circRNA mediates silica-induced macrophage activation via HECTD1/ZC3H12A-dependent ubiquitination. Theranostics. 2018;8(2):575–92. doi: 10.7150/thno.21648.

49. Liu H, Cheng Y, Yang J, Wang W, Fang S, Zhang W, et al. BBC3 in macrophages promoted pulmonary fibrosis development through inducing autophagy during silicosis. Cell death & disease. 2017;8(3):e2657.

doi: 10.1038/cddis.2017.78.

50. Liu H, Dai X, Cheng Y, Fang S, Zhang Y, Wang X, et al. MCPIP1 mediates silica-induced cell migration in human pulmonary fibroblasts. American journal of physiology Lung cellular and molecular physiology. 2015;310(2):L121–L32.

Figures

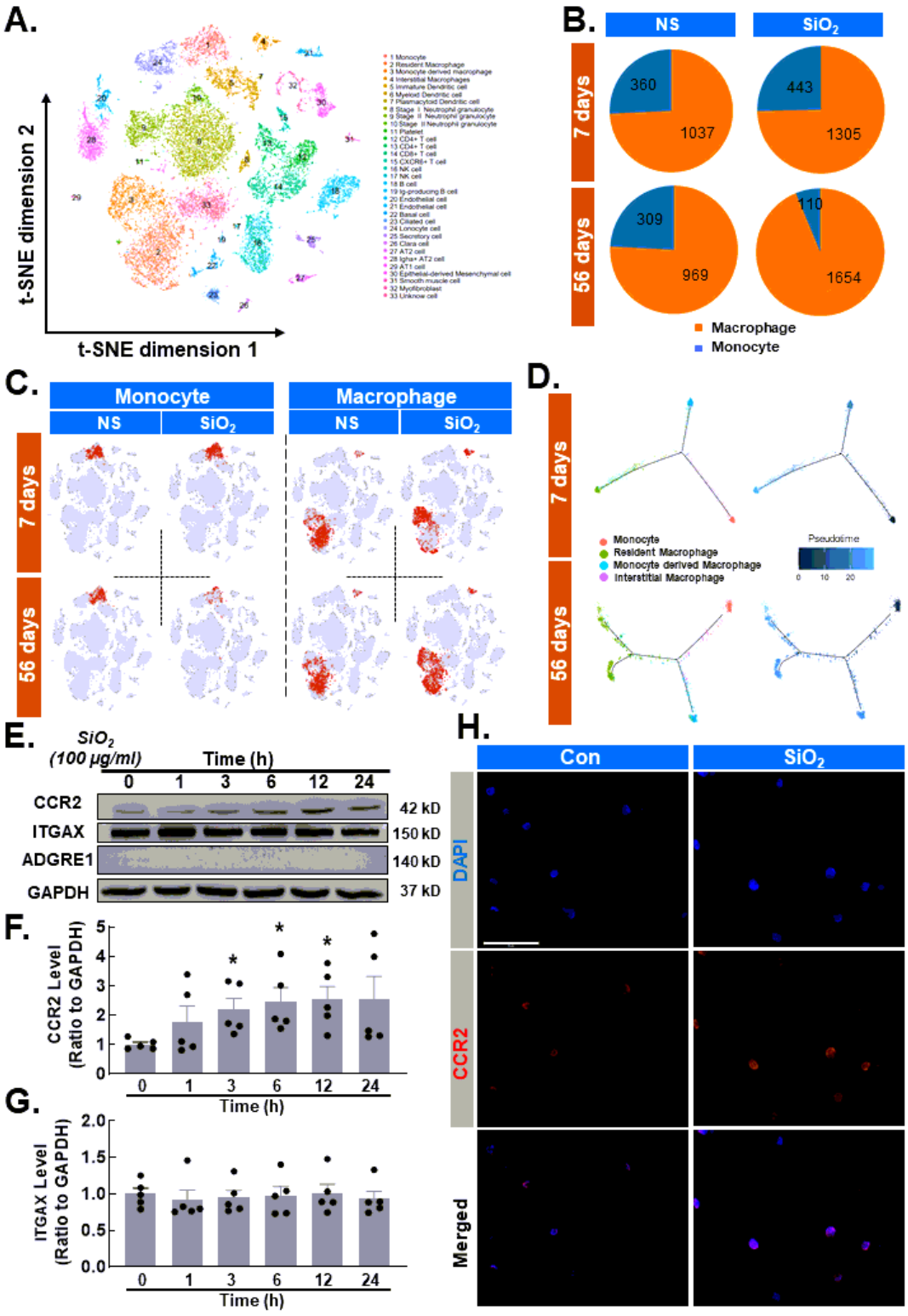

Figure 1

Silica promotes an infiltrating phenotype in monocytes. (A) Visualization of major classes of cells using *t*-SNE. Dots, individual cells; color, cell types. (B) Cell numbers and relative proportions of monocytes and macrophages are shown as pie charts at 7 d and 56 d. (C) As shown in the images, the monocyte numbers were decreased or showed no obvious difference in the SiO_2 group compared to the NC group, while macrophage numbers increased in the SiO_2 group. (D) Cell trajectory analysis of monocytes and

macrophages and pseudotime analysis. (E) Representative Western blot showing that SiO_2 induced CCR2 expression in a time-dependent manner in THP-1 cells. (F) Densitometric analyses of CCR2 levels from five independent experiments; *$P < 0.05$ compared with the 0 h group. (G) Densitometric analyses of ITGAX levels in five independent experiments. (H) Representative immunocytochemical staining images showing that SiO_2 induced CCR2 expression in THP-1 cells. Scale bar, 100 μm.

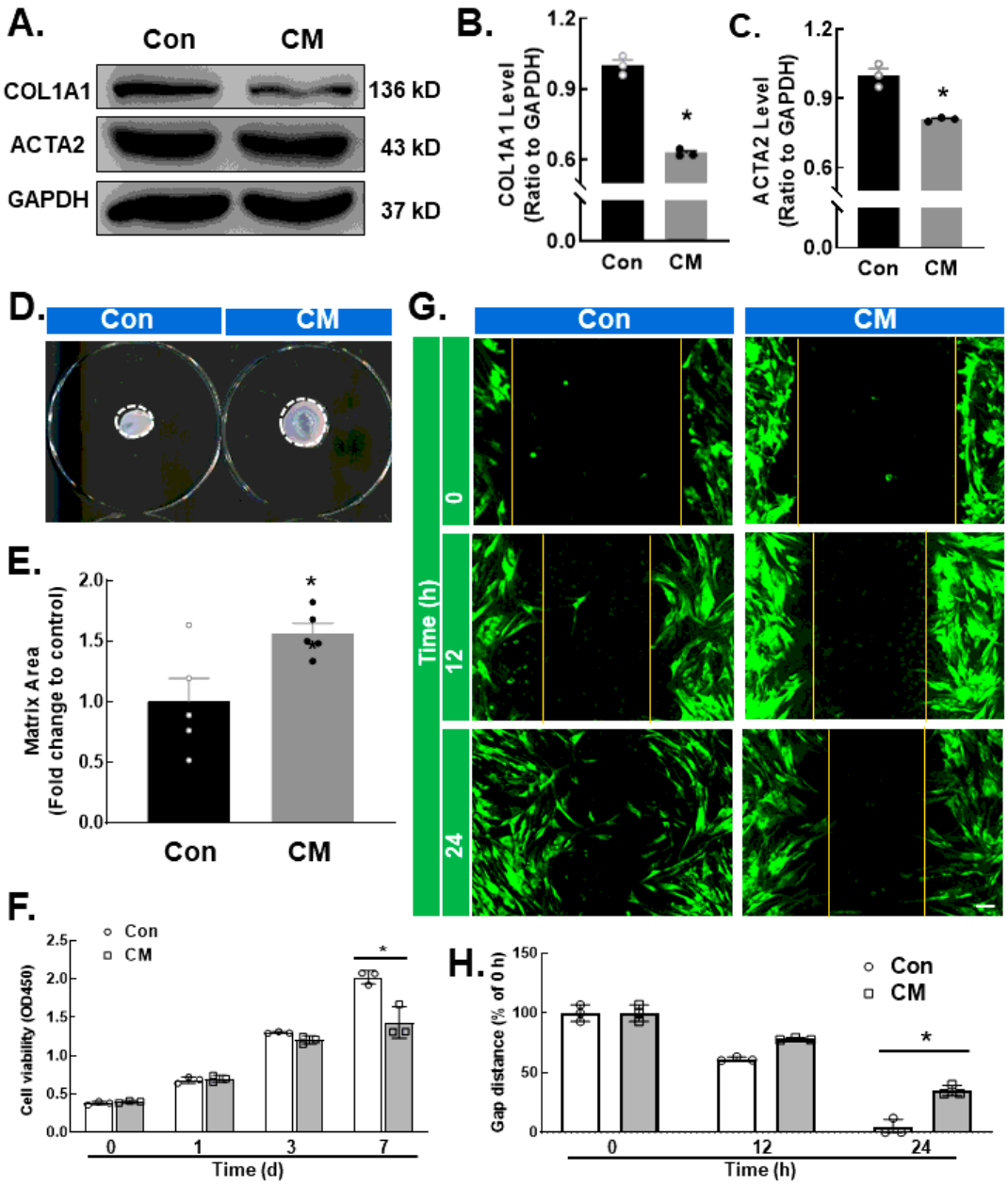

Figure 2

Monocytes play a negative role in fibroblast activation, migration and viability after silica treatment. (A) Representative Western blot showing the effect of CM on the upregulation of COL1A1 and ACTA2 in fibroblasts. (B) Densitometric analyses of COL1A1 levels in three independent experiments; *P < 0.05 vs. the control group. (C) Densitometric analyses of ACTA2 levels in three independent experiments; *P < 0.05 vs. the control group. (D) Representative images of the gel contraction assay of fibroblasts treated with CM. (E) Gel contraction assay results demonstrating the conditioned medium-induced decrease in fibroblasts; *P < 0.05 vs. the control group. (F) CCK-8 assay results showing that CM attenuated fibroblast viability; *P < 0.05 vs. the corresponding time point in the control group, n=3. (G) Representative images of a scratch assay showing that the migration of fibroblasts was attenuated by CM. Scale bar, 20 μm. (H) Quantification of the scratch gap distance in three independent experiments; *P < 0.05 vs. the corresponding time point in the control group.

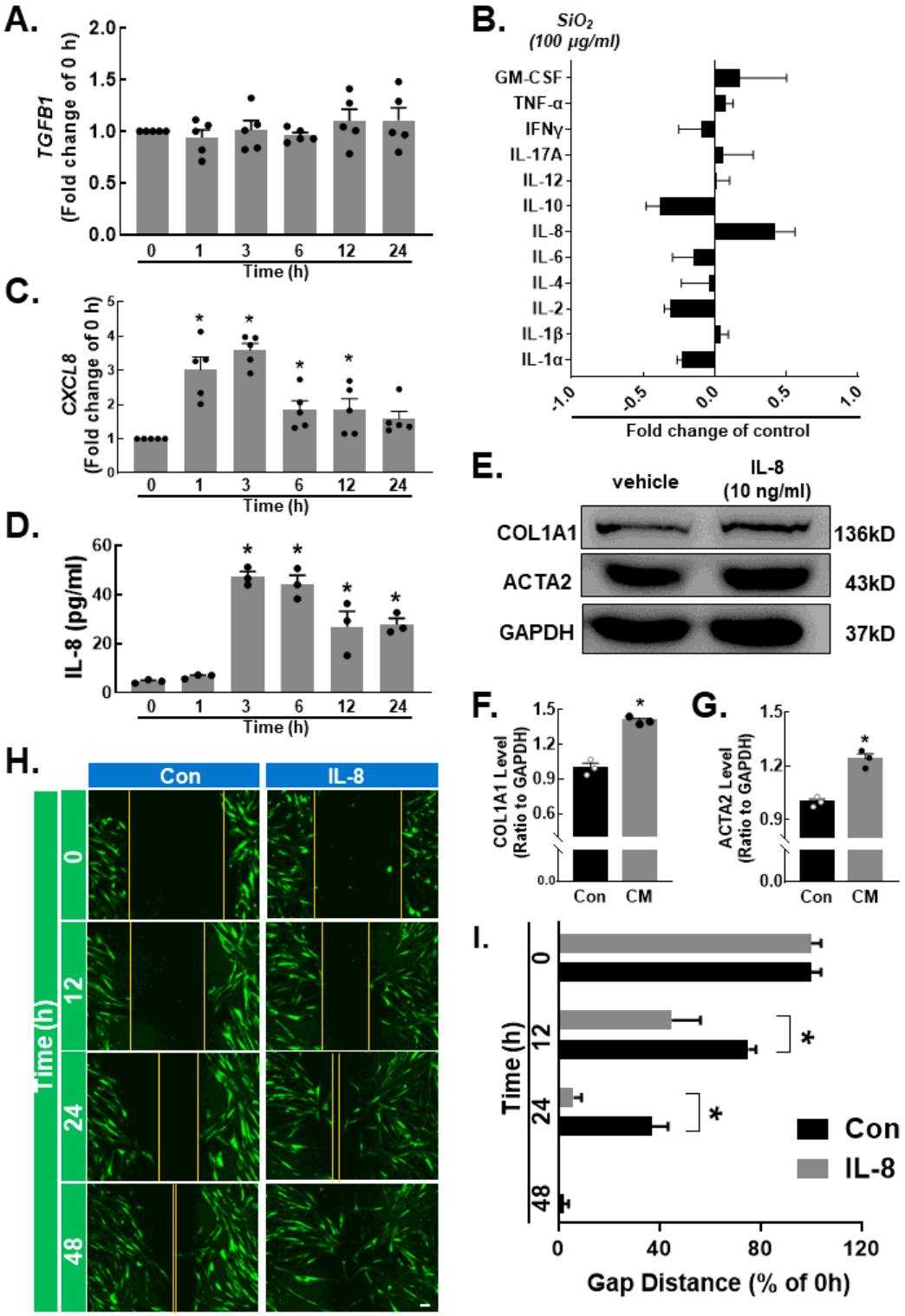

Figure 3

Increased IL-8 expression is not a key factor that affects fibroblast activation, viability and migration. (A) RT-qPCR analysis showed that SiO_2 stimulation had no effect on *TGFB1* expression. (B) SiO_2 induced the expression of 12 inflammatory factors in THP-1 cells. (C) RT-qPCR analysis showed that *cxcl8* expression was increased in THP-1 cells in response to SiO_2 stimulation (n=5); $*P < 0.05$ vs. the 0 h group. (D) ELISA analysis showed that IL-8 protein expression was increased in THP-1 cells in response to SiO_2 stimulation

(n=3); *P < 0.05 vs. the 0 h group. (E) Representative Western blot showing the effect of IL-8 on the upregulation of COL1A1 and ACTA2 in fibroblasts. (F) Densitometric analyses of COL1A1 protein expression levels in three independent experiments; *P < 0.05 vs. the control group. (G) Densitometric analyses of ACTA2 protein expression levels in three independent experiments; *P < 0.05 vs. the control group. (H) Representative images from the scratch assay showing that the migration of fibroblasts was increased by IL-8. Scale bar, 20 μm. (I) Quantification of the scratch gap distance in three independent experiments; *P < 0.05 vs. the corresponding time point in the control group.

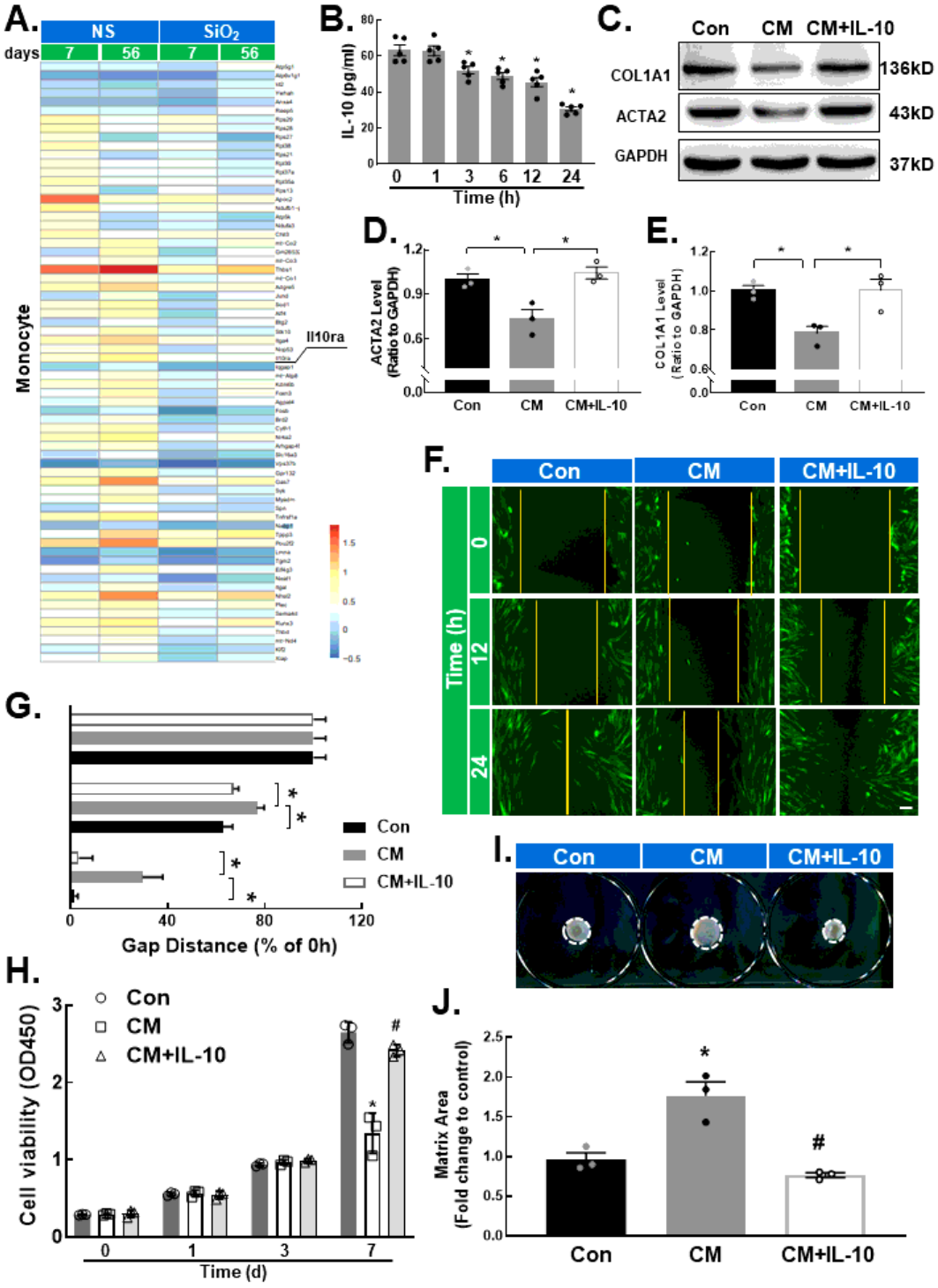

Figure 4

Decreased IL-10 release is a key factor that affects fibroblast activation, viability and migration. (A) IL10ra in the NS group and the SiO_2 group is shown in the heat map of the monocyte cluster. (B) ELISA analysis showed that SiO_2 decreased IL-10 protein expression in THP-1 cells (n=5); *P < 0.05 vs. the 0 h group. (C) Representative Western blot showing the effect of CM and IL-10 on the specific upregulation of COL1A1 and ACTA2 in fibroblasts. (D) Densitometric analyses of ACTA2 levels in three independent experiments; *P < 0.05 vs. the control group, *P < 0.05 vs. the CM group. (E) Densitometric analyses of COL1A1 levels in three independent experiments; *P < 0.05 vs. the control group, *P < 0.05 vs. the CM group. (F) Representative images from the scratch assay showing that the migration of fibroblasts was increased by CM and IL-10. Scale bar, 20 μm. (G) Quantification of the scratch gap distance in three independent experiments; *P < 0.05 vs. the corresponding time point in the control group. (H) CCK-8 assay results showing that fibroblast viability was increased by CM and IL-10; *P < 0.05 vs. the corresponding time point in the control group, #P < 0.05 vs. the corresponding time point in the CM group, n=3. (I) Representative images of gel contraction assays showing fibroblasts treated with CM and IL-10. (J) Gel contraction assay results demonstrating the decrease in fibroblast viability induced by CM and IL-10; *P < 0.05 vs. the control group, # P < 0.05 vs. the CM group, n=3.

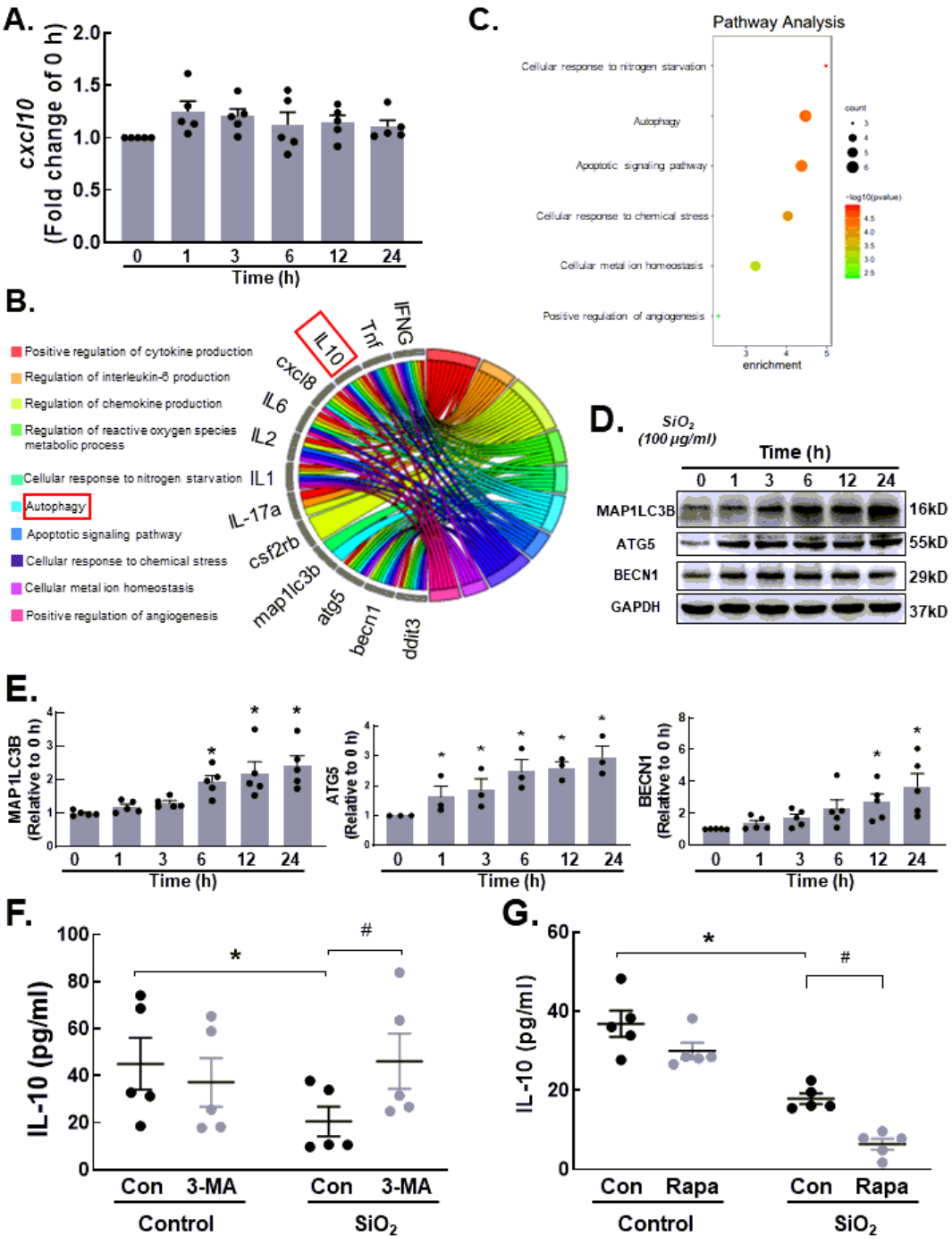

Figure 5

Autophagy is involved in the silica-induced reduction in IL-10 release by monocytes. (A) RT-qPCR analysis showed that SiO_2 stimulation had no effect on *cxcl10* expression. (B-C) As shown in the string map and bubble map, IL-10 plays an important role in autophagy signaling pathways. (D) Representative Western blot showing the effect of SiO_2 on the upregulation of MAP1LC3B, ATG5 and BECN1 in THP-1 cells. (E) Densitometric analyses of MAP1LC3B levels in five independent experiments; *$P < 0.05$ vs. the 0 h group.

Densitometric analyses of ATG5 levels in five independent experiments; *P < 0.05 vs. the 0 h group. Densitometric analyses of BECN1 levels in five independent experiments; *P < 0.05 vs. the 0 h group. (F) ELISA analysis showed that the SiO_2-induced reduction in IL-10 protein release by THP-1 cells was reversed by the autophagy blocker 3-MA (n=5), *P < 0.05 vs. the corresponding group in the control group. # P < 0.05 vs. the con group and the SiO_2 group. (G) ELISA analysis showed that the SiO_2-induced reduction in IL-10 protein release by THP-1 cells was promoted by the autophagy agonist rapamycin (n=5), *P < 0.05 vs. the corresponding group in the control group. # P < 0.05 vs. the con group and the SiO_2 group.

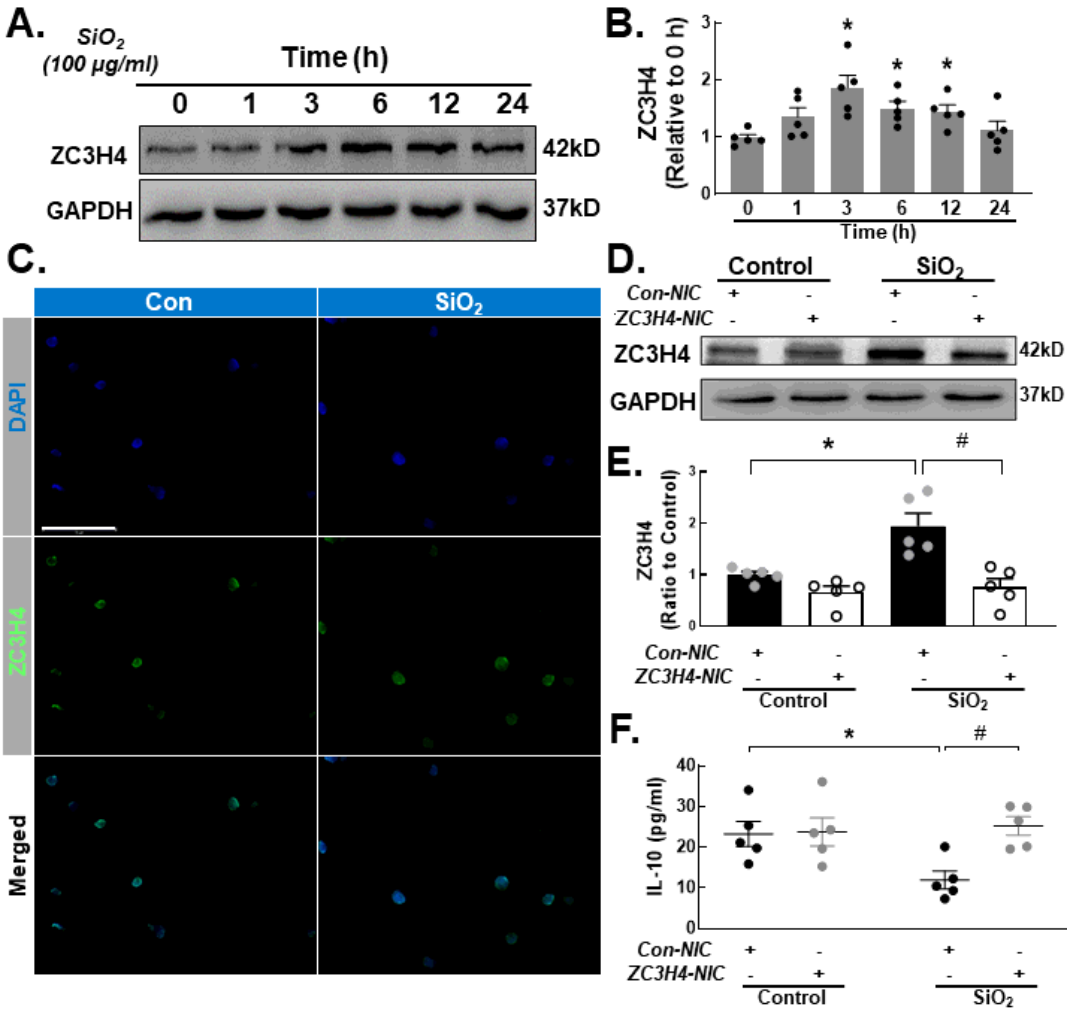

Figure 6

ZC3H4 is involved in regulating the silica-induced release of IL-10 by monocytes. (A) Representative Western blot showing that SiO_2 induced ZC3H4 expression in a time-dependent manner in THP-1 cells. (B) Densitometric analyses of ZC3H4 protein expression levels in five independent experiments; *P < 0.05 vs. the 0 h group. (C) Representative immunocytochemical staining images showing that SiO_2 induced ZC3H4 expression in THP-1 cells. Scale bar, 100 μm. (D) Representative Western blot showing that

ZC3H4 protein was knocked down in THP-1 cells after plasmid transfection. (E) Densitometric analyses of ZC3H4 protein expression levels in five independent experiments; *$P < 0.05$ vs. the corresponding group in the control group. # $P < 0.05$ vs. the Con-NIC^{+} ZC3H4-NIC^{-} group and the SiO_2 group. (F) ELISA analysis showed that knocking down the ZC3H4 protein increased IL-10 protein release by THP-1 cells. *$P < 0.05$ vs. the corresponding group and the control group. # $P < 0.05$ vs. the Con-NIC^{+} ZC3H4-NIC^{-} group and the SiO_2 group.

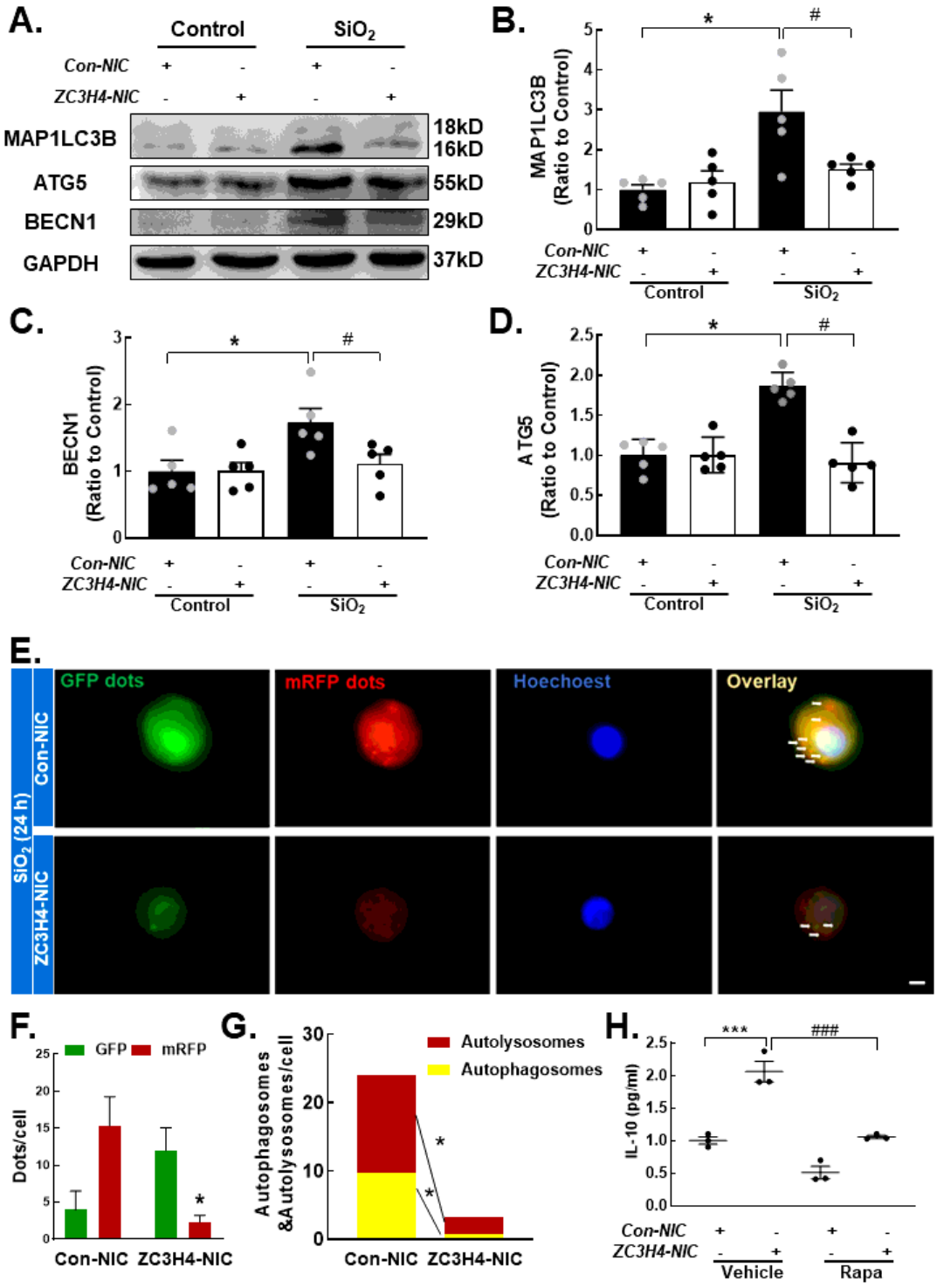

Figure 7

ZC3H4 regulates IL-10 release through autophagic processes. (A) Representative Western blot showing that knocking down ZC3H4 downregulated MAP1LC3B, ATG5 and BECN1 expression levels in THP-1 cells treated with SiO_2. (B) Densitometric analyses of MAP1LC3B protein expression levels in five independent experiments; *P < 0.05 vs. the corresponding group and the control group. # P < 0.05 vs. the Con-NIC$^+$ ZC3H4-NIC$^-$ group and the SiO_2 group. (C) Densitometric analysis of BECN1 protein expression levels in five independent experiments; *P < 0.05 vs. the corresponding group and the control group. # P < 0.05 vs. the Con-NIC$^+$ ZC3H4-NIC$^-$ group and the SiO_2 group. (D) Densitometric analysis of ATG5 protein expression levels in five independent experiments; *P < 0.05 vs. the corresponding group and the control group. # P < 0.05 vs. the Con-NIC+ ZC3H4-NIC- group and the SiO_2 group. (E) Representative images of the fluorescence map showing that autophagy was attenuated in THP-1 cells stimulated with SiO_2 and ZC3H4 protein knockdown. Scale bar, 80 μm. (F) Quantification of autophagy levels in THP-1 cells treated with SiO2 after ZC3H4 protein knockdown; *P < 0.05 vs. the corresponding color in the CON-NIC group. (G) Quantification of autolysosomes and autophagosomes in THP-1 cells treated with SiO2 after ZC3H4 protein knockdown; *P < 0.05 vs. the corresponding color in the CON-NIC group. (H) ELISA analysis showed that the autophagy agonist rapamycin decreased IL-10 protein release in THP-1 cells treated with SiO2 after ZC3H4 protein knockdown. ***P < 0.001 vs. the Con-NIC$^+$ Rapa$^-$ group. ### P < 0.001 vs. the NIC$^+$ Rapa$^-$ group.

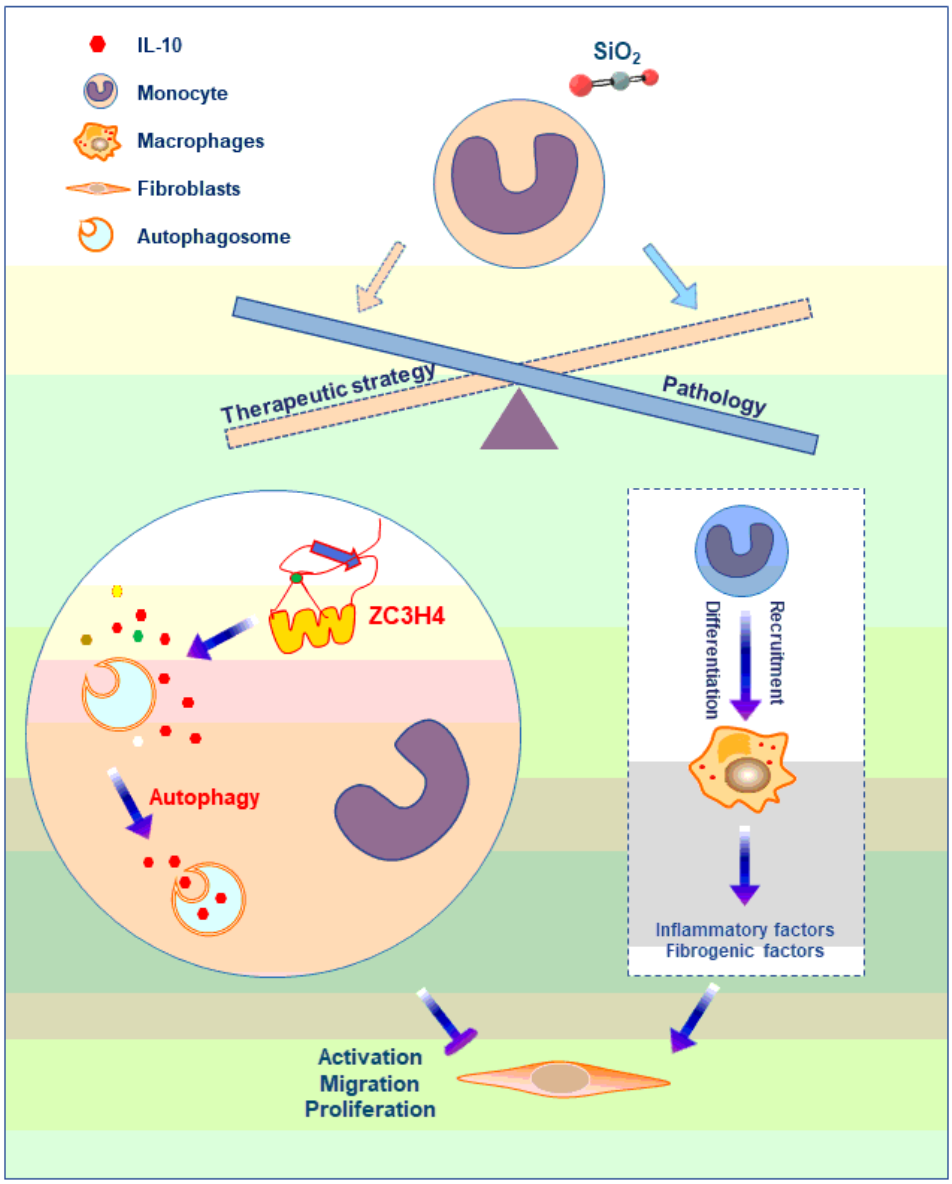

Figure 8

Schematic diagram showing that infiltrating monocytes can inhibit fibroblast activation, viability and migration and then inhibit lung fibrosis in the context of silicosis. ZC3H4 is a crucial protein associated with silicosis that can regulate IL-10 release by controlling autophagy in monocytes. Consequently, the regulation of monocyte differentiation might be a potential therapeutic strategy for inhibiting inflammation and fibrosis and would bring new opportunities for the treatment of silicosis.

Supplementary Files

This is a list of supplementary files associated with this preprint. Click to download.

- 2019MonocytesuppleYFHv3.docx